Published in final edited form as:
J Comp Neurol. 2014 August 1; 522(11): 2465–2480. doi:10.1002/cne.23583.

Differential LRRK2 Expression in the Cortex, Striatum, and Substantia Nigra in Transgenic and Nontransgenic Rodents

Andrew B. West[1,*], **Rita M. Cowell**[2,*], **João P.L. Daher**[1], **Mark S. Moehle**[1], **Kelly M. Hinkle**[3], **Heather L. Melrose**[3], **David G. Standaert**[1], and **Laura A. Volpicelli-Daley**[1]

[1]Center for Neurodegeneration and Experimental Therapeutics and Department of Neurology, University of Alabama at Birmingham, Birmingham, AL 35294

[2]Department of Psychiatry & Behavioral Neurobiology, University of Alabama at Birmingham, Birmingham, AL 35294

[3]Department of Neuroscience, Mayo Clinic Jacksonville, Jacksonville FL, 32224, USA

Abstract

Mutations in *leucine-rich repeat kinase 2* (*LRRK2)* are found in a significant proportion of late-onset Parkinson's disease (PD) patients. Elucidating the neuroanatomical localization of LRRK2 will further define LRRK2 function and the molecular basis of PD. Here, we utilize recently characterized monoclonal antibodies to evaluate LRRK2 expression in rodent brain regions relevant to PD. In both mice and rats, LRRK2 is highly expressed in the cortex and striatum, particularly in pyramidal neurons of layer V and in medium spiny neurons within striosomes. Overall, rats have a more restricted distribution of LRRK2 compared to mice. Mice, but not rats, show high levels of LRRK2 expression in the substantia nigra pars compacta. Expression of the pathogenic LRRK2-G2019S protein from mouse BAC constructs closely mimics endogenous LRRK2 distribution in the mouse brain. However, LRRK2-G2019S expression derived from human BAC constructs causes LRRK2 to be expressed in additional neuron subtypes in the rat such as striatal cholinergic interneurons and the substantia nigra pars compacta. The distribution of LRRK2 from human BAC constructs more closely resembles descriptions of LRRK2 in humans and non-human primates. Computational analyses of DNA regulatory elements in LRRK2 show a primate-specific promoter sequence that does not exist in lower mammalian species. These non-coding regions may be involved in directing neuronal expression patterns. Together, these studies will aid in understanding the normal function of LRRK2 in the brain and will assist in model selection for future studies.

Corresponding author information: Andrew West, 1719 6th Ave S., Birmingham, AL 35294, Phone (205 996-7697), Fax (205 996-6580), abwest@uab.edu.
*indicates equal contribution

All authors declare no conflict of interest.

Author Contributions. All authors had full access to all the data in the study and take responsibility for the integrity of the data and the accuracy of the data analysis. Study concept and design: A.B.W., R.M.C., L.V.D. Acquisition of data: L.V.D., R.M.C., A.B.W., J.P.L.D., M.S.M., K.M.H.; Drafting of the manuscript: A.B.W., L.V.D.; Critical revision of the manuscript for important intellectual content: A.B.W., L.V.D., R.M.C., H.L.M., D.G.S.; Obtained funding: A.B.W., H.L.M.; Administrative, technical and material support: A.B.W, R.M.C., H.L.M., J.P.L.D., M.S.M., K.M.H., L.V.D.; Study supervision: A.B.W., L.V.D.

Keywords

Parkinson's disease; Neurodegeneration; Nigrostriatal Circuit; Bacterial-artificial Chromosome (BAC) transgenics

Introduction

Autosomal-dominant missense mutations in the *leucine-rich repeat kinase 2* gene (*LRRK2*) produce a strong susceptibility to PD with symptoms associated with late-onset disease (Paisan-Ruiz et al., 2004; Zimprich et al., 2004). Understanding the normal function of LRRK2 and the consequences of the mutations will help to elucidate the neurobiological basis of PD. Furthermore, because the protein kinase domain of LRRK2 has successfully been targeted by small molecule inhibitors *in vitro*, LRRK2 represents one of the most promising novel targets for therapeutics (West et al., 2005; Cookson, 2010).

Rodent models provide an important tool for understanding the etiology of PD and for screening of novel neuroprotective pharmacological treatments. Transgenic bacterial artificial chromosome (BAC) mice have been developed harboring LRRK2 mutations associated with PD, in particular the most common G2019S familial mutation. One of the major transgenic lines developed include mice overexpressing murine LRRK2 under the control of the endogenous murine LRRK2 promoter (Li et al., 2010). PD-relevant phenotypes from mice with LRRK2 expression driven from human BAC constructs have also been described (Li et al., 2009). The recent development of BAC transgenic rats harboring human LRRK2 G2019S mutations provide an additional tool for studying the contribution of LRRK2 to PD susceptibility (see Methods section for details regarding this strain). Characterization of rat models in PD may be important in pre-clinical studies for experimental therapeutics since physiology is easier to monitor as compared to mice, behavioral tests of motor function and learning and memory are well established, and surgical procedures are often easier due to the larger size of the rat. However, LRRK2 expression or localization in the brain has not yet been described in rats or in transgenic rats.

A substantial body of evidence implicates abnormalities in striatonigral circuits in PD in motor behavior (DeLong and Wichmann, 2007), and more recent studies suggest a role for cortical dysfunction in cognitive and executive function decline (Irwin et al., 2012). Characterizing the neuroanatomical localization of LRRK2 in the brain in non-transgenic and transgenic rodent models is crucial for understanding how LRRK2 may play a role in brain circuitry, pathogenic functions, and subsequent development of LRRK2 directed therapies. However, to date, the neuroanatomical localization of LRRK2 has been challenging because of a lack of sensitive and specific antibodies, and the lack of suitable LRRK2 knockout (KO) animals to serve as appropriate controls (Davies et al., 2013). Recently, a consortium led by the West laboratory and the Melrose laboratory was formed to systematically characterize ten monoclonal antibodies targeting LRRK2 in brain tissue (Davies et al., 2013). Here, we capitalize upon these studies and use highly specific LRRK2 antibodies, together with knockout animals side-by-side, to ensure specificity, to perform a comparative analysis of LRRK2 distribution in the striatum, cortex, and substantia nigra

pars compacta (SNpc) in several strains of rodents. Importantly, all critical reagents described in this study are commercially available, and it is hoped that this baseline information on LRRK2 distribution will assist in interpreting existing literature describing these rodents as well as the design of future studies enabled because of the unique and differential LRRK2 localization in different strains and species.

Methods

Antibody Characterization

See table 1 for details on antibodies used in this study.

The two antibodies used for the localization of LRRK2 (N241A/34 and c41-2) have been characterized previously (Davies et al., 2013). The LRRK2 N241A/34 mouse monoclonal antibody (NeuroMab, 73-253) was raised against an active recombinant LRRK2 fragment (amino acids 970-2527). This antibody produced a single band corresponding to LRRK2 from mouse and rat brain lysates, with no detectable bands (resulting from primary antibody signal) in lysates from LRRK2 knockout (LRRK2-KO) brains (Davies et al., 2013). The anatomical distribution of LRRK2 immunohistochemistry using mouse brain sections in this study resembled the pattern seen for LRRK2 mRNA (Melrose et al., 2006; Simon-Sanchez et al., 2006a; Higashi et al., 2007; Giesert et al., 2013). All experimental observations of LRRK2 presented here were matched together with tissue sections from LRRK2-KO mice, processed in parallel, to ensure signal for LRRK2 was specific. The N241A/34 mouse monoclonal antibody was not prioritized for immunohistochemical detection of LRRK2 in mouse brain owing to the increased background observed (in both WT and KO mice) due to secondary antibody cross detection of endogenous mouse proteins.

Previously, the LRRK2 c41-2 rabbit monoclonal antibody (Epitomics, 3514-1) was found to detect a predominant band corresponding to LRRK2 in immunoblots from wild type and not LRRK2-KO mouse brain lysates (Davies et al., 2013). This LRRK2 antibody was also raised against the active recombinant LRRK2 fragment (amino acids 970-2527). The anatomical distribution of LRRK2 immunohistochemistry using c41-2 resembled the pattern seen for LRRK2 mRNA previously published. Under conditions described here, no signal was apparent in tissue sections from LRRK2-KO mice using antibody c41-2 in sections processed in parallel with WT or transgenic strains. The c41-2 antibody was not prioritized for immunohistochemical detection of LRRK2 in rat brain, since in some areas of the rat brain, c41-2 detected cells consistent with the morphology of astrocytes in both WT and LRRK2-KO rats (Davies et al., 2013), although in all observations in this work, c41-2 signal could reproduce the staining in neurons observed in rats using the N241A/34 antibody.

The calbindin rabbit monoclonal antibody (Epitomics, 2946-1) predominantly labeled matrix regions in the striatum in rats and mice used here, as previously demonstrated for calbindin distribution as a canonical marker for the matrix (Gerfen, 1989; Liu and Graybiel, 1992). The antibody was generated in rabbits with an N-terminal fragment of calbindin from amino acids 1-150, affinity purified and produces a single band by western blot of ~30kDa (Manufacturer's datasheet). The MOR-1 (μ-opioid receptor, OPRM1) rabbit monoclonal antibody (Epitomics, 3675-1) predominantly labeled striosomes in the striatum in both rats

and mice used here as previously described (Atweh and Kuhar, 1977; Gerfen, 1984). The antibody was generated in rabbits with a C-terminal fragment of MOR-1 corresponding to amino acids 250–400, and recognizes a single band by western blot of ~75kDa (Manufacturer's datasheet). Although both antibodies have not been validated in knockout animals for their respective target, or previously published (to our knowledge), the striking concentration of LRRK2 in the striosomes and matrix produced by these antibodies in the rat and mouse striatum, similar to previous reports, suggest specificity of signal.

The GAD67, TH, parvalbumin, α-synuclein, ChAT, and DARPP-32 antibodies used here can be found in the current version of the JCN antibody database. The mouse IgG2a affinity purified monoclonal anti-GAD67 (Millipore, MAB5406) was generated using full length human GAD67 as immunogen, and the manufacturer reports no cross reactivity with GAD65 by western blot and immunostaining in the rat hippocampus consistent with expected distribution (Manufacturer's datasheet). The rabbit polyclonal anti-TH antibody (Santa Cruz, H-196) was generated by immunizing rabbits with an N-terminal recombinant human TH protein (amino acids 1-196) and generates a single band of 60 kDa by western blot (Manufacturer's datasheet). The TH antibody produces expected anatomical distribution in the striatum and substantia nigra in both rats and mice. The mouse IgG1 monoclonal targeting α-synuclein (BD Biosciences, 610785) was generated with recombinant protein consisting of amino acids 15–123 of rat α-synuclein protein. The antibody detects a single band by western blot of ~20 kDa (Manufacturer's datasheet) and the expected pre-synaptic distribution in the rats and mice was observed in this study. The polyclonal affinity purified anti-choline acetyltransferase antibody was developed in a goat with purified human placental choline acetyltransferase as immunogen. The Manufacturer reports staining of rat neocortex and rat septal organotypic slice cultures with the distribution expected for choline acetyltransferase positive neurons, and we observe the strong expected interneuron staining in rats and mice striatum used in this study. Finally, affinity purified rabbit monoclonal antibody anti-DARPP-32 (Cell Signaling, 19A3) produces a single band by western blot of the expected size in mouse and rat brain, and no bands were detected in the DARPP-32 knockout mouse brain (Manufacturer's datasheet). In addition, the Manufacturer reports the expected distribution of cells stained with this antibody in the striatum, and expected distribution of cells in the striatum, retina and cerebellum.

Animals

All animal protocols were approved by the Authors' respective Institutional Animal Care and Use Committee and were in accordance with the National Institute of Health Guide for the Care and Use of Laboratory Animals (NIH Publications No. 80-23). All mice used were male, 8 to 12 weeks of age. The murine BAC LRRK2-G2019 mice are available from the Jackson Laboratory and were developed in the laboratory of Zhenyu Yue (Li et al., 2010) and have been bred with C57Bl/6J inbred mice for at least 10 generations. The Sprague-Dawley human BAC LRRK2 G2019S rat strain was developed in the laboratory of Dr. Chenjian Li, and sponsored by the Michael J. Fox Foundation for deposition to Taconic farms and has undergone at least 3 generations of breeding by the vendor on the outbred line of Sprague-Dawley (Charles Rivers). The BAC LRRK2 G2019S rat strain, to our knowledge, has not been described in the literature, but a related strain, and details of the

generation and characterization of the BAC LRRK2 R1441G rat have been published (Li et al., 2009).

LRRK2 knockout (KO) lines on mice were exon 41 deleted mice on a C57BL/6 background developed by Melrose and Farrer ((Hinkle et al., 2012); the Jackson Laboratory) with undetectable LRRK2 protein and no truncated LRRK2 products detected by immunoblot. LRRK2 KO rats on a Long-Evans Hooded outbred background were developed by Sigma Advanced Genetic Engineering Labs, via targeted genomic editing to introduce a 10 base pair deletion in exon 30 via Zinc-Finger Nuclease technology. This deletion results in an early frame shift and the resultant transcript is degraded by non-sense mediated decay, with no detectable LRRK2 protein (Davies et al., 2013). A Tg(Th-eGFP)DJ76Gsat transgenic mouse was obtained from Jackson laboratory, originally developed by the GENSAT brain atlas of gene expression program, and has been previously described (Ibanez-Sandoval et al., 2010) (Moehle et al., 2012).

Rodent brain free-floating immunohistochemistry

Observations in this study were made from 12 male WT and 12 male LRRK2 KO (Hinkle et al., 2012) mice aged 4 months, and 12 male WT and 12 male LRRK2 KO rats aged 2–4 months. Similar group sizes were used for LRRK2-BAC transgenic mice and rats. Individual experiments presented here are representative of at least three animals per group. Animals were terminally anesthetized with ketamine and xylazine cocktail (120/20mg/kg for mice, 75/10mg/kg for rats) and transcardially perfused 0.9% saline with 10U/mL heparin followed by ice cold 4% PFA. Brains were dissected and post-fixed at 4°C for 2 hours in 4% PFA, then transferred to 30% sucrose in PBS at 4°C for cryopreservation. Once saturated in sucrose, brains were flash frozen in isopentane cooled on dry ice and stored −80°C until sectioning at 40 μm on a sledge microtome (Leica). Sections were rinsed 3 times with Tris-buffered saline (TBS). All rinses and primary and secondary antibody diluents were in TBS. For DAB detection only, sections were pre-quenched with 3% H_2O_2 for 10 minutes followed by 3 rinses. To enable antigen retrieval, all sections were incubated with 10 mM sodium citrate, pH 6.0, containing 0.05% Tween-20 for 30 minutes at 37°C with agitation. Following x3 5 minute washes, non-specific sites were blocked by incubating sections for 1 hr in 5% normal serum from the host of the secondary antibody containing 0.3% triton X-100 (with 10 Og/mL avidin for DAB) at 4°C with agitation. Following 3 rinses, sections were incubated in primary antibody diluted in 5% normal serum (with 50 Og/mL biotin for DAB) for 24–48 hrs. “No primary” antibody and concentration and species-matched IgG controls were included in each experiment. Sections were washed 3 times for 5 minutes and then placed in secondary antibody in 5% normal serum 18 hr at 4°C with agitation. Secondary antibodies include: biotinylated goat anti- mouse (Vector Laboratories, Burlingame, CA); donkey anti-rabbit or anti-mouse (CF555, CF488, Sigma-Aldrich, St. Louis, MO); goat anti-mouse IgG1 or IgG2a specific (Alexa 488, Alexa 555, Life Technologies, Grand Island, NY). The next day, sections were washed 3 times. Sections for fluorescence were mounted using Prolong Gold (Life Technologies, Grand Island, NY). For DAB, sections were incubated with Avidin-Biotin Complex reagent (Vector Labs) for 30 minutes, washed 3 times again, then developed in 3,3′-diaminobenzidine (DAB) substrate or ImmPACT substrate (Vector Labs, Burlingame, CA) for 2–5 minutes. The sections were

placed in distilled water to terminate the DAB development reaction and mounted with 25% ethanol in PBS onto positively charged glass slides (ThermoFisher). Following at least 3 hours of air drying, the slides were dehydrated in ascending alcohols and three changes of xylene and coverslipped with Permount (ThermoFisher).

We obtained the highest LRRK2 signal over background in immunohistochemistry experiments when freshly sectioned brain sections were used the same day as perfusions, and PFA post-fixation was limited to 24 hours or less. LRRK2 signal precipitously declined with storage of brain sections at 4°C or −20°C, with most signal lost after just a few days in both rats and mice. Thus, LRRK2 is unusually sensitive to storage conditions. For the data presented here, all attempts were made to stain as fresh as sections as possible, although storage of whole-frozen and cryopreserved brains at −80°C had smaller deleterious effects and LRRK2 signal could be recovered from brains stored at −80°C for several weeks to months.

Microscopy

Confocal images were captured using a Leica TCS-SP5 laser-scanning confocal microscope. The Leica LASAF software, Adobe Photoshop (contrast, brightness and color adjustments), and Adobe Illustrator were used to create figures and process images. Images from sections stained with DAB were captured using a Zeiss AxioObserver.Z1 microscope.

Immunoblotting

Male mice were terminally anesthetized with isofluorane and euthanized by decapitation for removal of the brain, and dissection of brain regions was performed. Tissue was homogenized directly into Laemmli buffer supplemented with a protease inhibitor cocktail (Roche Diagnostics Corporation, Indianapolis, IN). Lysates were directly loaded onto 7.5% TGX (Bio-rad) polyacrylamide gels and electrophoresed at 10V/cm for ~1.5 hours. Acrylamide gels of 10% or less are suitable for resolution and transfer of LRRK2 protein; higher percentages impede complete LRRK2 transfer to membranes. SDS-PAGE gels were combined with either activated PVDF or nitrocellulose (Millipore), with equivalent results, into Tris-Glycine transfer buffer overnight at 35V at 4°C. Membranes were washed and successful protein transfer and equality of loading verified with Ponceau S (Sigma) stain. Membranes were blocked in Tris-buffered saline/0.1% Tween-20 (TBS-T) with 5% skimmed milk or 5% bovine serum albumin (BSA, approximate equivalent results obtained using either BSA or milk as a blocking reagent for the antibodies described here) for 1 hour and primary antibody was applied overnight at 4°C or for 1–2 hours at room temperature (RT).

Promoter analysis

All genome sequences were obtained from the UCSC Genome Bioinformatics portal. LRRK2 regulatory sequences were retrieved through alignment of the first coding exon of LRRK2, and this assignment agreed with the cDNA and predicted transcriptional start of LRRK2 in all species evaluated here. BLASTn (NCBI) and BLAT (UCSC Genome Bioinformatics portal) tools were used for global alignment. mVISTA (available through the Genomics Division of Lawrence Berkeley National Laboratory and US Department of

Energy Joint Genome Institute) was used for sequence alignment, with LAGAN alignments and Shuffle-LAGAN alignments utilized as described (Brudno et al., 2003).

Results

LRRK2 in rodent striatum

Recently, we demonstrated the specificity of the mouse monoclonal LRRK2 antibody, N241/34A, by both immunoblot and immunohistochemistry, and showed that this antibody recognizes both mouse and rat LRRK2 (Davies et al., 2013). Using this antibody, we found that LRRK2 was expressed in the striatum in both rat and mouse brain (Figure 1A), where it was enriched in striosomes (also called patches; Figure 1B), as has been demonstrated previously for mouse LRRK2 using a rabbit polyclonal antibody that does not recognize rat LRRK2 (Mandemakers et al., 2012). However, the relative level of enrichment of LRRK2 expression in rat striosomes was much more pronounced than in mouse striatum. Double labeling immunofluorescence in rats showed that LRRK2 is enriched in striosomes labeled using MOR-1 (Figure 1C) (Atweh and Kuhar, 1977; Gerfen, 1984). LRRK2 expression was much lower in the calbindin-positive matrix (Figure 1D)(Liu and Graybiel, 1992). Throughout the striatum in both rats and mice, LRRK2 expression appeared to be restricted to cells with the location and size of medium spiny neurons, with low to undetectable expression in larger interneurons (Figure 1E).

Higher magnification images in striosomes showed localization of LRRK2 to neuropil puncta and within cell bodies of medium spiny neurons (Figure 2). Although TH-positive dopaminergic terminals and fibers were found juxtaposed to LRRK2 puncta, LRRK2 immunofluorescence did not colocalize with TH, suggesting that LRRK2 does not localize to these TH positive axons in either rats or mice (Figure 2A). LRRK2-positive medium spiny neuron cell bodies were surrounded by terminals positive for GAD67, and parvalbumin which are expressed predominantly by striatal interneurons that were devoid of LRRK2 expression in rats and mice (Figure 2B, E). Furthermore, no instances of overlap between LRRK2 and the pre-synaptic protein α-synuclein could be detected (Figure 2C). Since α-synuclein is a robust and broad marker for presynaptic terminals, these data suggest the majority of LRRK2 localizes to the somatodendritic domains of medium spiny neurons. However, additional ultrastructural localization experiments are required to pinpoint the identity of these domains.

The MOR-1 receptor localizes to extrasynaptic sites within medium spiny neuron dendrites (Kaneko et al., 1995; Wang et al., 1996; 1997). Within striosomes enriched for both LRRK2 and MOR-1, neuropil puncta for both proteins never co-localized but were exquisitely juxtaposed, forming pairs in many instances and suggesting assignment of LRRK2 puncta to a proportion of post-synaptic sites in the striosomes (Figure 2D). LRRK2 likewise did not overlap with parvalbumin, a calcium buffer concentrated in fast-spiking interneurons; parvalbumin-positive terminals were observed surrounding medium spiny neurons with LRRK2 staining throughout the soma (Figure 2E). Finally, DARPP-32 staining in the neuronal perikarya in the striatum overlapped with LRRK2 positive neuronal perikarya (Figure 2F), confirming the medium spiny localization of LRRK2.

LRRK2 Localization in Rodent Motor Cortex

In the rat cortex (Figure 1A1), LRRK2 immunoreactivity was not as abundant as in the striatum, in contrast to mouse cortex, which exhibited LRRK2 immunoreactivity throughout all cortical layers (Figure 1A2). Higher magnification images (Figure 3A) in the motor cortex showed LRRK2 localized primarily to pyramidal projection neurons in layer V in the rat, whereas LRRK2 immunoreactivity was found in neurons throughout all cortical layers in mouse (Figure 4B). LRRK2 localized to apical dendrites, but LRRK2 never overlapped with α-synuclein expression (Figure 3C,D). As expected of a dominant pre-synaptic protein, α-synuclein immunoreactivity was restricted to terminals contacting the perikarya and apical dendrites of layer V pyramidal neurons (Figure 3D).

LRRK2 Expression in the Rodent SNpc

Whether LRRK2 protein and/or mRNA is expressed in the cells selectively vulnerable in PD, namely dopaminergic neurons in the SNpc, has been a contentious issue, with studies both confirming expression in these cells and also failing to detect expression (Biskup et al., 2006; Galter et al., 2006; Simon-Sanchez et al., 2006b; Taymans et al., 2006; Melrose et al., 2007). With the descriptions of several anti-LRRK2 polyclonal antibodies, LRRK2 protein expression was described in the mouse and human SNpc (Biskup et al., 2006; Giasson et al., 2006; Greggio et al., 2006; Higashi et al., 2007; Melrose et al., 2007). Here, with the benefit of more sensitive monoclonal antibodies and the availability of LRRK2 KO animals as a comparison group, we confirm expression of LRRK2 in mouse dopaminergic neurons, but fail to detect any signal for LRRK2 using similar staining conditions in rat dopaminergic neurons in the SNpc (Figure 4A).

To confirm with a second method that LRRK2 is expressed in dopaminergic neurons in the mouse SNpc, we utilized a mouse strain developed in the GeneSat project that expresses eGFP from a BAC construct harboring the TH gene, as previously described (Gong et al., 2003). In eGFP-positive neurons of the mouse SNpc (Figure 4B), LRRK2 expression primarily localized to neuronal perikarya, with weaker neuropil puncta than in the striatum and very little dendritic localization as compared to LRRK2 positive neurons in the cortex. In contrast, in rat midbrain sections (Figure 4C) imagined with confocal analysis, no LRRK2 immunoreactivity could be observed in TH positive neurons. In addition, LRRK2 showed minimal expression in the abutting substantia nigra pars reticulata (Figure 4A) in both rats and mice.

While overall comparable LRRK2 intensities in WT mice are observed with LRRK2 positive cells in the cortex, striatum and SNpc, in rats, LRRK2 expression in the striatum was obviously higher than that of the SNpc where LRRK2 could not be detected. To help determine whether it is possible to detect any LRRK2 expression in the rat SNpc, we titrated the LRRK2 primary antibody (N241A/34), starting with our standard concentration of 1 μg/ml to a high concentration of 40 μg/ml (Figure 5). For these experiments, the secondary concentration was held constant. Only at the highest concentration of anti-LRRK2 antibody (40 μg/ml) could any signal in the rat SNpc be discerned. While the overall signal intensity increased in the LRRK2 KO sections that were processed in parallel with the highest concentrations of antibody (right side panels, Figure 5), no specific cells in the SNpc could

be detected. Together with serial sections processed in parallel with anti-TH antibody and morphological markers provided by Nissl contrast stain, these results suggest detectable but very low levels of LRRK2 in the WT rat SNpc.

LRRK2 Distribution in BAC-Expressing Transgenic Rodents

We next investigated the pattern of expression of LRRK2 in transgenic mice harboring the LRRK2-G2019S gene encoded within a mouse-genome derived BAC construct (Li et al., 2010). Exogenous LRRK2-G2019S expression is thus driven from the native mouse promoter sequence. Immunoblots of LRRK2 from LRRK2-G2019S BAC mice relative to nontransgenic C57BL/6J control mice show a 20–30 fold increase in LRRK2 expression across the brain (Figure 6A,B). Upon immunohistochemical analysis, the LRRK2-G2019S BAC mice still showed the highest levels of expression in the cortex and striatum, with clear expression in the SNpc (Figure 6C,D). Similar patterns of expression were observed in the layers of the cortex, striosomes in the striatum, with still a lack of clear LRRK2 expression in the substantia nigra pars reticulata. Thus, the transgenic mice display remarkable overlap with the distribution observed in nontransgenic mice, even in the context of substantial over-expression.

Recently, Sprague-Dawley rats harboring LRRK2-G2019S encoded from a human-genome derived BAC construct were released commercially by Taconic Farms. Immunoblots again show an approximately 20–30 fold increase in LRRK2 expression in the human LRRK2-G2019S BAC transgenic rats relative to nontransgenic rats, similar to the mouse LRRK2-G2019S transgenic mice (Figure 7A,B). Overall, expression of LRRK2 remained the highest in the cortex and striatum in the transgenic rats. However, using the N241/34A antibody which recognizes both rat and human LRRK2 with similar affinities (Davies et al., 2013), we found distinct differences in LRRK2 distribution in these animals compared to LRRK2 protein endogenously expressed in nontransgenic rat brains. Unlike the restricted localization to Layer V of the cortex in nontransgenic rats, LRRK2 in LRRK2-G2019S human BAC rats was intensely expressed across layers II–V, in neurons of various morphologies (Figure 7C). In the midbrain, LRRK2 became intensely expressed in dopaminergic (TH positive) neurons of the SNpc where it co-localized with TH (Figure 7D). Still, no significant LRRK2 signal could be detected in the substantia nigra reticulata. In the striatum, there were scattered intensely LRRK2-positive neurons (in fact, the most intensely labeled neurons that we could find across the entire brain). These were large and polygonal and often located on the edge of striosomes, suggestive of cholinergic interneurons (Figure 7E), The cholinergic nature of these were confirmed by dual labeling with an antibody to choline-acetyltransferase (Figure 7F). In contrast, parvalbumin-positive interneurons showed low LRRK2 expression in the BAC transgenic rats (Figure 7G).

Lack of Conservation of the LRRK2 Promoter in Mammals

To begin to elucidate the mechanisms by which nontransgenic rodent LRRK2 and human BAC LRRK2 transgenic animals show such dramatic differences in the patterns of expression, we examined *LRRK2* DNA regulatory elements (i.e., DNA sequence surrounding exon 1 of the *LRRK2* gene). The nucleotides of the open-reading frame encoding the LRRK2 protein are highly conserved in mammals, with over 80% nucleotide

sequence identity in rats and mice compared to human (BLAST analysis), and over 90% conservation in non-human primates compared with human. The amino acid sequence of the LRRK2 protein is also highly conserved, with over 88% identity between rats, mice and humans, and more than 95% conservation between humans and non-human primates. However, the same is not true for the regulatory regions in LRRK2. A basic-local alignment search of 4 kilobases of sequence upstream of human exon 1 reveals that this sequence bears no significant homology to any genomic sequences known in rats or mice, and many other lower mammalian species, using standard filters for local alignment quality (e.g., UCSC BLAT or NCBI BLAST tools). As this is unusual for sequence within conserved genes between rodents and humans, we used more specialized bioinformatics approaches designed to align sequences from more evolutionarily distant species. We found that fragments of the human LRRK2 promoter can be detected in rats and mice, but these sequences were subject to heavy inversion, rearrangements and recombination, as visualized using a Shuffle-LAGAN alignment (Figure 8A). As expected, remnants of the first transcribed exon can be detected in all mammals evaluated, but otherwise there is not a consistent regulatory region that remains highly conserved in mammals. Areas of significant sequence deviation can also be detected even between rats and mice, two species that usually have a very high overall conservation of gene-encoding regions (Figure 8B). Thus, while the LRRK2 protein sequence itself is highly conserved in mammals, the regulatory regions outside of the coding exons are dissimilar and have been subject to intense recombination within mammalian evolution. It is possible that differential LRRK2 localization patterns we observed in this study arise because of inter-species differences in regulatory elements, driven heavily by evolutionary selection processes.

Discussion

The development of mammalian model systems is critical for understanding and potentially treating the underpinnings of complex diseases like PD (Lee et al., 2012). Mutations in LRRK2 represent the most common known genetic cause of late-onset PD (Ross et al., 2011), yet descriptions of what types of cells actually express LRRK2 protein natively in the mouse and human brain have been relatively vague, and even divergent in some cases. Descriptions of LRRK2 distribution in the most commonly used LRRK2 transgenic mice have also been incomplete. Finally, LRRK2 distribution in the rat brain has not been previously described to our knowledge, yet rats can be important pre-clinical models of neurodegeneration with advantages over mice in some areas of translational research. Our goal for this study was to provide a comparative analysis of LRRK2 in brain regions that are most routinely evaluated in PD research, in both rats and mice, and transgenic strains of rodents that express pathogenic LRRK2 protein.

In the cortex, striatum, and SNpc, the pattern of LRRK2 expression differs in distinct neuronal subtypes between rats and mice. Arguably the most important of these differences with respect to PD research is the differential LRRK2 expression in the dopaminergic neurons in the SNpc. In mice, LRRK2 expression can be readily detected in the SNpc with both immunofluorescence and DAB immunohistochemistry. Likewise, LRRK2 is found in human dopaminergic SNpc cells (Greggio et al., 2006; Higashi et al., 2007). In nontransgenic rats, there was no LRRK2 signal in TH positive SNpc cells. However, in rats

that express LRRK2 protein driven by a human promoter from a BAC construct, LRRK2 becomes highly expressed in dopaminergic SNpc neurons.

Furthermore, in transgenic rats with a human LRRK2 BAC construct, other neurons, such as cholinergic interneurons in the striatum, become highly LRRK2 positive. LRRK2 distribution in the transgenic rats becomes more reminiscent of descriptions of LRRK2 in non-human primates and human brain, for example high levels of LRRK2 in striatal interneurons (Higashi et al., 2007; Lee et al., 2010). In the case of striatal interneurons, this phenomenon is not likely to be a result of simple overexpression in the transgenic rats because overexpression of LRRK2 from a murine promoter produces a pattern of staining similar to nontransgenic rodents.

In transgenic or nontransgenic rats and mice, LRRK2 localizes to neurons that could modify processing of cortical-striatal inputs. In particular, the striatum predominantly receives projections from Layer V of the cortex, an area in which LRRK2 is enriched. It has been shown that Layer V afferents preferentially synapse in MOR1-enriched striosomes where we can show LRRK2 concentrates, which in turn send afferents to the SNpc (Gerfen 1984), yet another area of LRRK2 expression (but only in mice and transgenic rats). Furthermore, striosomes also have been shown to primarily receive inputs from the allocortex which includes the olfactory bulb and hippocampus, other brain areas in which LRRK2 is expressed (Biskup et al., 2006; Melrose et al., 2007; Winner et al., 2011). It is noteworthy that in human PD, these brain areas are also dense with α-synuclein containing Lewy bodies and Lewy neurites, the primary pathological hallmarks of PD (Churchyard and Lees, 1997; Duda et al., 2002; Braak et al., 2003). Recent emerging evidence suggests interactions between LRRK2 and α-synuclein aggregation (Lin et al., 2009; Orenstein et al., 2013), but this remains controversial (Daher et al., 2012; Herzig et al., 2012). Thus, the cortico-striatal circuit may in part be selectively vulnerable in PD because of the concentration of proteins known to underlie aspects of late-onset PD.

At a subcellular level, in striatal and cortical neurons, LRRK2 appears primarily within soma and dendrites and shows no overlap with presynaptic markers. Rather, close associations with MOR-1 puncta and TH-positive projections suggest a dominant post-synaptic localization in the striatum. Although LRRK2 has been shown to play a role in presynaptic vesicle endo/exocytosis (Belluzzi et al., 2012), our data suggest an additional, perhaps more predominant, functional role for LRRK2 in the soma and dendrites. Ultimately, detailed electron microscopy studies will be needed to pinpoint LRRK2 within neurons. Based on our initial observations, LRRK2 subcellular distribution on an electron microscopy level may be quite different between neuronal subtypes, for example layer V projection neurons with prominent apical dendritic localization and perinuclear puncta, or striatal medium spiny neurons with post-synaptic localization, or in dopaminergic SNpc neurons that show diffuse perikarya localization.

The LRRK2 protein sequence itself is highly conserved, with reasonable protein homologs found in even single-celled organisms (Marin, 2006). However, analyses of 5′ upstream (i.e., regulatory) regions of the *LRRK2* gene reveal marked differences across species and very poor conservation within mammals. We hypothesize that part of the explanation for

differential cellular LRRK2 distribution in the mammalian brain may be due to these species-specific elements. Further dissection of these regulatory regions may reveal new classes of DNA regulatory elements that drive expression in unique subclasses of neurons.

Overall, we hope our findings may aid in determining the normal function of LRRK2 in the brain and in selecting rodent models for particular experiments to study how pathogenic LRRK2 mutations might contribute to disease.

Supplementary Material

Refer to Web version on PubMed Central for supplementary material.

Acknowledgments

The work was supported by: NIH R01NS064934, U18NS082132, R01NS065860, Michael J. Fox Foundation for Parkinson's Disease Research, American Parkinson's Disease Association.

The authors would like to thank Nour Sukar and Jonathan Blackburn for their excellent technical assistance.

References

Atweh SF, Kuhar MJ. Autoradiographic localization of opiate receptors in rat brain. III. The telencephalon. Brain Res. 1977; 134(3):393–405. [PubMed: 198065]

Belluzzi E, Greggio E, Piccoli G. Presynaptic dysfunction in Parkinson's disease: a focus on LRRK2. Biochem Soc Trans. 2012; 40(5):1111–1116. [PubMed: 22988874]

Biskup S, Moore DJ, Celsi F, Higashi S, West AB, Andrabi SA, Kurkinen K, Yu SW, Savitt JM, Waldvogel HJ, Faull RL, Emson PC, Torp R, Ottersen OP, Dawson TM, Dawson VL. Localization of LRRK2 to membranous and vesicular structures in mammalian brain. Annals of neurology. 2006; 60(5):557–569. [PubMed: 17120249]

Braak H, Del Tredici K, Rub U, de Vos RA, Jansen Steur EN, Braak E. Staging of brain pathology related to sporadic Parkinson's disease. Neurobiol Aging. 2003; 24(2):197–211. [PubMed: 12498954]

Brudno M, Do CB, Cooper GM, Kim MF, Davydov E, Program NCS, Green ED, Sidow A, Batzoglou S. LAGAN and Multi-LAGAN: efficient tools for large-scale multiple alignment of genomic DNA. Genome research. 2003; 13(4):721–731. [PubMed: 12654723]

Churchyard A, Lees AJ. The relationship between dementia and direct involvement of the hippocampus and amygdala in Parkinson's disease. Neurology. 1997; 49(6):1570–1576. [PubMed: 9409348]

Cookson MR. The role of leucine-rich repeat kinase 2 (LRRK2) in Parkinson's disease. Nat Rev Neurosci. 2010; 11(12):791–797. [PubMed: 21088684]

Daher JP, Pletnikova O, Biskup S, Musso A, Gellhaar S, Galter D, Troncoso JC, Lee MK, Dawson TM, Dawson VL, Moore DJ. Neurodegenerative phenotypes in an A53T alpha-synuclein transgenic mouse model are independent of LRRK2. Hum Mol Genet. 2012; 21(11):2420–2431. [PubMed: 22357653]

Davies P, Hinkle KM, Sukar NN, Sepulveda B, Mesias R, Serrano G, Alessi DR, Beach TG, Benson DL, White CL, Cowell RM, Das SS, West AB, Melrose HL. Comprehensive characterization and optimization of anti-LRRK2 (leucine-rich repeat kinase 2) monoclonal antibodies. Biochem J. 2013; 453(1):101–113. [PubMed: 23560750]

DeLong MR, Wichmann T. Circuits and circuit disorders of the basal ganglia. Arch Neurol. 2007; 64(1):20–24. [PubMed: 17210805]

Duda JE, Giasson BI, Mabon ME, Lee VM, Trojanowski JQ. Novel antibodies to synuclein show abundant striatal pathology in Lewy body diseases. Ann Neurol. 2002; 52(2):205–210. [PubMed: 12210791]

Galter D, Westerlund M, Carmine A, Lindqvist E, Sydow O, Olson L. LRRK2 expression linked to dopamine-innervated areas. Ann Neurol. 2006; 59(4):714–719. [PubMed: 16532471]

Gerfen CR. The neostriatal mosaic: compartmentalization of corticostriatal input and striatonigral output systems. Nature. 1984; 311(5985):461–464. [PubMed: 6207434]

Gerfen CR. The neostriatal mosaic: striatal patch-matrix organization is related to cortical lamination. Science. 1989; 246(4928):385–388. [PubMed: 2799392]

Giasson BI, Covy JP, Bonini NM, Hurtig HI, Farrer MJ, Trojanowski JQ, Van Deerlin VM. Biochemical and pathological characterization of Lrrk2. Ann Neurol. 2006; 59(2):315–322. [PubMed: 16437584]

Giesert F, Hofmann A, Burger A, Zerle J, Kloos K, Hafen U, Ernst L, Zhang J, Vogt-Weisenhorn DM, Wurst W. Expression analysis of Lrrk1, Lrrk2 and Lrrk2 splice variants in mice. PLoS One. 2013; 8(5):e63778. [PubMed: 23675505]

Gong S, Zheng C, Doughty ML, Losos K, Didkovsky N, Schambra UB, Nowak NJ, Joyner A, Leblanc G, Hatten ME, Heintz N. A gene expression atlas of the central nervous system based on bacterial artificial chromosomes. Nature. 2003; 425(6961):917–925. [PubMed: 14586460]

Greggio E, Jain S, Kingsbury A, Bandopadhyay R, Lewis P, Kaganovich A, van der Brug MP, Beilina A, Blackinton J, Thomas KJ, Ahmad R, Miller DW, Kesavapany S, Singleton A, Lees A, Harvey RJ, Harvey K, Cookson MR. Kinase activity is required for the toxic effects of mutant LRRK2/dardarin. Neurobiol Dis. 2006; 23(2):329–341. [PubMed: 16750377]

Herzig MC, Bidinosti M, Schweizer T, Hafner T, Stemmelen C, Weiss A, Danner S, Vidotto N, Stauffer D, Barske C, Mayer F, Schmid P, Rovelli G, van der Putten PH, Shimshek DR. High LRRK2 levels fail to induce or exacerbate neuronal alpha-synucleinopathy in mouse brain. PLoS One. 2012; 7(5):e36581. [PubMed: 22615783]

Higashi S, Biskup S, West AB, Trinkaus D, Dawson VL, Faull RL, Waldvogel HJ, Arai H, Dawson TM, Moore DJ, Emson PC. Localization of Parkinson's disease-associated LRRK2 in normal and pathological human brain. Brain research. 2007; 1155:208–219. [PubMed: 17512502]

Hinkle KM, Yue M, Behrouz B, Dachsel JC, Lincoln SJ, Bowles EE, Beevers JE, Dugger B, Winner B, Prots I, Kent CB, Nishioka K, Lin WL, Dickson DW, Janus CJ, Farrer MJ, Melrose HL. LRRK2 knockout mice have an intact dopaminergic system but display alterations in exploratory and motor coordination behaviors. Mol Neurodegener. 2012; 7:25. [PubMed: 22647713]

Ibanez-Sandoval O, Tecuapetla F, Unal B, Shah F, Koos T, Tepper JM. Electrophysiological and morphological characteristics and synaptic connectivity of tyrosine hydroxylase-expressing neurons in adult mouse striatum. The Journal of neuroscience : the official journal of the Society for Neuroscience. 2010; 30(20):6999–7016. [PubMed: 20484642]

Irwin DJ, White MT, Toledo JB, Xie SX, Robinson JL, Van Deerlin V, Lee VM, Leverenz JB, Montine TJ, Duda JE, Hurtig HI, Trojanowski JQ. Neuropathologic substrates of Parkinson disease dementia. Ann Neurol. 2012; 72(4):587–598. [PubMed: 23037886]

Kaneko T, Minami M, Satoh M, Mizuno N. Immunocytochemical localization of mu-opioid receptor in the rat caudate-putamen. Neuroscience letters. 1995; 184(3):149–152. [PubMed: 7715834]

Lee H, Melrose HL, Yue M, Pare JF, Farrer MJ, Smith Y. Lrrk2 localization in the primate basal ganglia and thalamus: a light and electron microscopic analysis in monkeys. Exp Neurol. 2010; 224(2):438–447. [PubMed: 20483355]

Lee Y, Dawson VL, Dawson TM. Animal models of Parkinson's disease: vertebrate genetics. Cold Spring Harb Perspect Med. 2012; 2(10)

Li X, Patel JC, Wang J, Avshalumov MV, Nicholson C, Buxbaum JD, Elder GA, Rice ME, Yue Z. Enhanced striatal dopamine transmission and motor performance with LRRK2 overexpression in mice is eliminated by familial Parkinson's disease mutation G2019S. The Journal of neuroscience : the official journal of the Society for Neuroscience. 2010; 30(5):1788–1797. [PubMed: 20130188]

Li Y, Liu W, Oo TF, Wang L, Tang Y, Jackson-Lewis V, Zhou C, Geghman K, Bogdanov M, Przedborski S, Beal MF, Burke RE, Li C. Mutant LRRK2(R1441G) BAC transgenic mice recapitulate cardinal features of Parkinson's disease. Nature neuroscience. 2009; 12(7):826–828.

Lin X, Parisiadou L, Gu XL, Wang L, Shim H, Sun L, Xie C, Long CX, Yang WJ, Ding J, Chen ZZ, Gallant PE, Tao-Cheng JH, Rudow G, Troncoso JC, Liu Z, Li Z, Cai H. Leucine-rich repeat kinase

2 regulates the progression of neuropathology induced by Parkinson's-disease-related mutant alpha-synuclein. Neuron. 2009; 64(6):807–827. [PubMed: 20064389]

Liu FC, Graybiel AM. Heterogeneous development of calbindin-D28K expression in the striatal matrix. J Comp Neurol. 1992; 320(3):304–322. [PubMed: 1351896]

Mandemakers W, Snellinx A, O'Neill MJ, de Strooper B. LRRK2 expression is enriched in the striosomal compartment of mouse striatum. Neurobiol Dis. 2012; 48(3):582–593. [PubMed: 22850484]

Marin I. The Parkinson disease gene LRRK2: evolutionary and structural insights. Mol Biol Evol. 2006; 23(12):2423–2433. [PubMed: 16966681]

Melrose H, Lincoln S, Tyndall G, Dickson D, Farrer M. Anatomical localization of leucine-rich repeat kinase 2 in mouse brain. Neuroscience. 2006; 139(3):791–794. [PubMed: 16504409]

Melrose HL, Kent CB, Taylor JP, Dachsel JC, Hinkle KM, Lincoln SJ, Mok SS, Culvenor JG, Masters CL, Tyndall GM, Bass DI, Ahmed Z, Andorfer CA, Ross OA, Wszolek ZK, Delldonne A, Dickson DW, Farrer MJ. A comparative analysis of leucine-rich repeat kinase 2 (Lrrk2) expression in mouse brain and Lewy body disease. Neuroscience. 2007; 147(4):1047–1058. [PubMed: 17611037]

Moehle MS, Webber PJ, Tse T, Sukar N, Standaert DG, DeSilva TM, Cowell RM, West AB. LRRK2 inhibition attenuates microglial inflammatory responses. The Journal of neuroscience : the official journal of the Society for Neuroscience. 2012; 32(5):1602–1611. [PubMed: 22302802]

Orenstein SJ, Kuo SH, Tasset I, Arias E, Koga H, Fernandez-Carasa I, Cortes E, Honig LS, Dauer W, Consiglio A, Raya A, Sulzer D, Cuervo AM. Interplay of LRRK2 with chaperone-mediated autophagy. Nature neuroscience. 2013; 16(4):394–406.

Paisan-Ruiz C, Jain S, Evans EW, Gilks WP, Simon J, van der Brug M, Lopez de Munain A, Aparicio S, Gil AM, Khan N, Johnson J, Martinez JR, Nicholl D, Carrera IM, Pena AS, de Silva R, Lees A, Marti-Masso JF, Perez-Tur J, Wood NW, Singleton AB. Cloning of the gene containing mutations that cause PARK8-linked Parkinson's disease. Neuron. 2004; 44(4):595–600. [PubMed: 15541308]

Ross OA, Soto-Ortolaza AI, Heckman MG, Aasly JO, Abahuni N, Annesi G, Bacon JA, Bardien S, Bozi M, Brice A, Brighina L, Van Broeckhoven C, Carr J, Chartier-Harlin MC, Dardiotis E, Dickson DW, Diehl NN, Elbaz A, Ferrarese C, Ferraris A, Fiske B, Gibson JM, Gibson R, Hadjigeorgiou GM, Hattori N, Ioannidis JP, Jasinska-Myga B, Jeon BS, Kim YJ, Klein C, Kruger R, Kyratzi E, Lesage S, Lin CH, Lynch T, Maraganore DM, Mellick GD, Mutez E, Nilsson C, Opala G, Park SS, Puschmann A, Quattrone A, Sharma M, Silburn PA, Sohn YH, Stefanis L, Tadic V, Theuns J, Tomiyama H, Uitti RJ, Valente EM, van de Loo S, Vassilatis DK, Vilarino-Guell C, White LR, Wirdefeldt K, Wszolek ZK, Wu RM, Farrer MJ. Association of LRRK2 exonic variants with susceptibility to Parkinson's disease: a case-control study. Lancet Neurol. 2011; 10(10):898–908. [PubMed: 21885347]

Simon-Sanchez J, Herranz-Perez V, Olucha-Bordonau F, Perez-Tur J. LRRK2 is expressed in areas affected by Parkinson's disease in the adult mouse brain. Eur J Neurosci. 2006a; 23(3):659–666. [PubMed: 16487147]

Simon-Sanchez J, Marti-Masso JF, Sanchez-Mut JV, Paisan-Ruiz C, Martinez-Gil A, Ruiz-Martinez J, Saenz A, Singleton AB, Lopez de Munain A, Perez-Tur J. Parkinson's disease due to the R1441G mutation in Dardarin: a founder effect in the Basques. Mov Disord. 2006b; 21(11):1954–1959. [PubMed: 16991141]

Taymans JM, Van den Haute C, Baekelandt V. Distribution of PINK1 and LRRK2 in rat and mouse brain. J Neurochem. 2006; 98(3):951–961. [PubMed: 16771836]

Wang H, Moriwaki A, Wang JB, Uhl GR, Pickel VM. Ultrastructural immunocytochemical localization of mu opioid receptors and Leu5-enkephalin in the patch compartment of the rat caudate-putamen nucleus. The Journal of comparative neurology. 1996; 375(4):659–674. [PubMed: 8930791]

Wang H, Moriwaki A, Wang JB, Uhl GR, Pickel VM. Ultrastructural immunocytochemical localization of mu-opioid receptors in dendritic targets of dopaminergic terminals in the rat caudate-putamen nucleus. Neuroscience. 1997; 81(3):757–771. [PubMed: 9316027]

West AB, Moore DJ, Biskup S, Bugayenko A, Smith WW, Ross CA, Dawson VL, Dawson TM. Parkinson's disease-associated mutations in leucine-rich repeat kinase 2 augment kinase activity.

Proceedings of the National Academy of Sciences of the United States of America. 2005; 102(46): 16842–16847. [PubMed: 16269541]

Winner B, Melrose HL, Zhao C, Hinkle KM, Yue M, Kent C, Braithwaite AT, Ogholikhan S, Aigner R, Winkler J, Farrer MJ, Gage FH. Adult neurogenesis and neurite outgrowth are impaired in LRRK2 G2019S mice. Neurobiol Dis. 2011; 41(3):706–716. [PubMed: 21168496]

Zimprich A, Biskup S, Leitner P, Lichtner P, Farrer M, Lincoln S, Kachergus J, Hulihan M, Uitti RJ, Calne DB, Stoessl AJ, Pfeiffer RF, Patenge N, Carbajal IC, Vieregge P, Asmus F, Muller-Myhsok B, Dickson DW, Meitinger T, Strom TM, Wszolek ZK, Gasser T. Mutations in LRRK2 cause autosomal-dominant parkinsonism with pleomorphic pathology. Neuron. 2004; 44(4):601–607. [PubMed: 15541309]

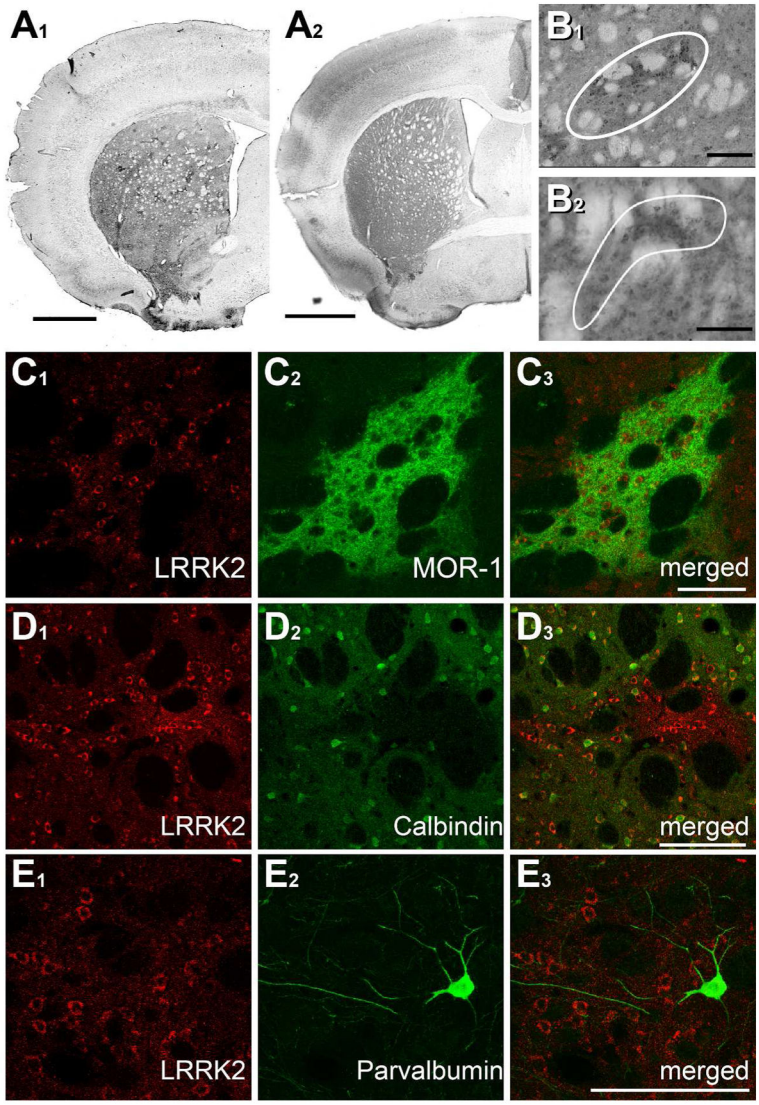

Figure 1. LRRK2 in adult rodent striatum

A) Monoclonal antibody N241A/34 (rat brain, panel A1) and c41-2 (mouse brain, panel A2) detection of LRRK2 in rodent sections using DAB immunohistochemistry. An anterior section of striatum is shown at comparable levels between mouse and rat. Comparable results were also obtained in serial sections using monoclonal antibody c41-2 in both species. Results are representative of at least pairs (WT with a KO control) of mice and rats processed. Scale bars are 1 mm. **B)** Higher magnification reveals intense LRRK2 signal enrichment (highlighted with a white surround) in striosomes, in rat coronal striatum sections (panel B1) and mouse coronal striatum sections (panel B2). The striosome enrichment in mouse is typically not as pronounced as in rat (relative to neighboring matrix LRRK2 staining). **C)** Double labeling immunofluorescence reveals enrichment of LRRK2 in MOR-1 positive striosomes in rat striatal sections. **D)** Calbindin staining shows inverse striosome (i.e., matrix) distribution. LRRK2 shows reduced signal (compared with striosome signal) in calbindin matrix staining in rat striatum. **E)** Shown is a parvalbumin positive

interneuron within a striosome from rat striatum. LRRK2 does not show any expression in parvalbumin interneurons. Scale bars for panels B–E are all 0.1 mm. A magenta-green version of the images is available as Supplemental Figure 1.

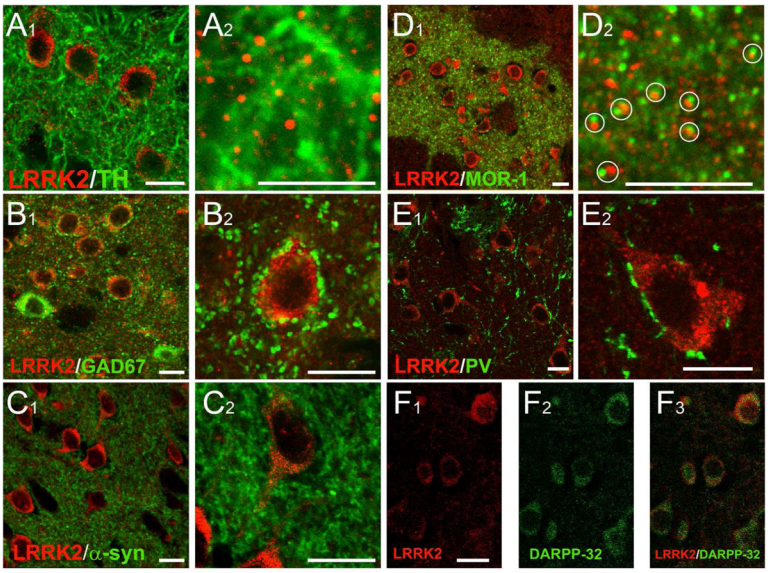

Figure 2. LRRK2 in wild-type adult rodent striatal neurons

In the anterior striatum of rats, **A)** no LRRK2 expression could be detected along TH positive fibers, but LRRK2 puncta were often directly juxtaposed to TH fibers, suggestive of LRRK2 being post-synaptic to dopaminergic input. **B)** LRRK2 signal was excluded from GAD67 positive interneurons, although GAD67 could be observed adjacent to LRRK2, suggesting GAD67 synapses on many LRRK2 positive soma. **C)** LRRK2 shows no overlap with the presynaptic marker, α-synuclein, and similar to GAD67, α-synuclein could be observed adjacent to LRRK2 positive neurons. **D)** LRRK2 signal outside of neuronal perikarya did not overlap with MOR-1, but rather formed pairs with MOR-1 puncta (prominent pairs highlighted with white circles). **E)** An 86 nm thick confocal slice showing intense parvalbumin (PV)-positive terminals adjacent to LRRK2-positive neurons. **F)** An 86 nm thick confocal slice showing overlap between LRRK2 and DARPP-32 in striatal neurons. Scale bars are all 10 μm. A magenta-green version of the images is available as Supplemental Figure 2.

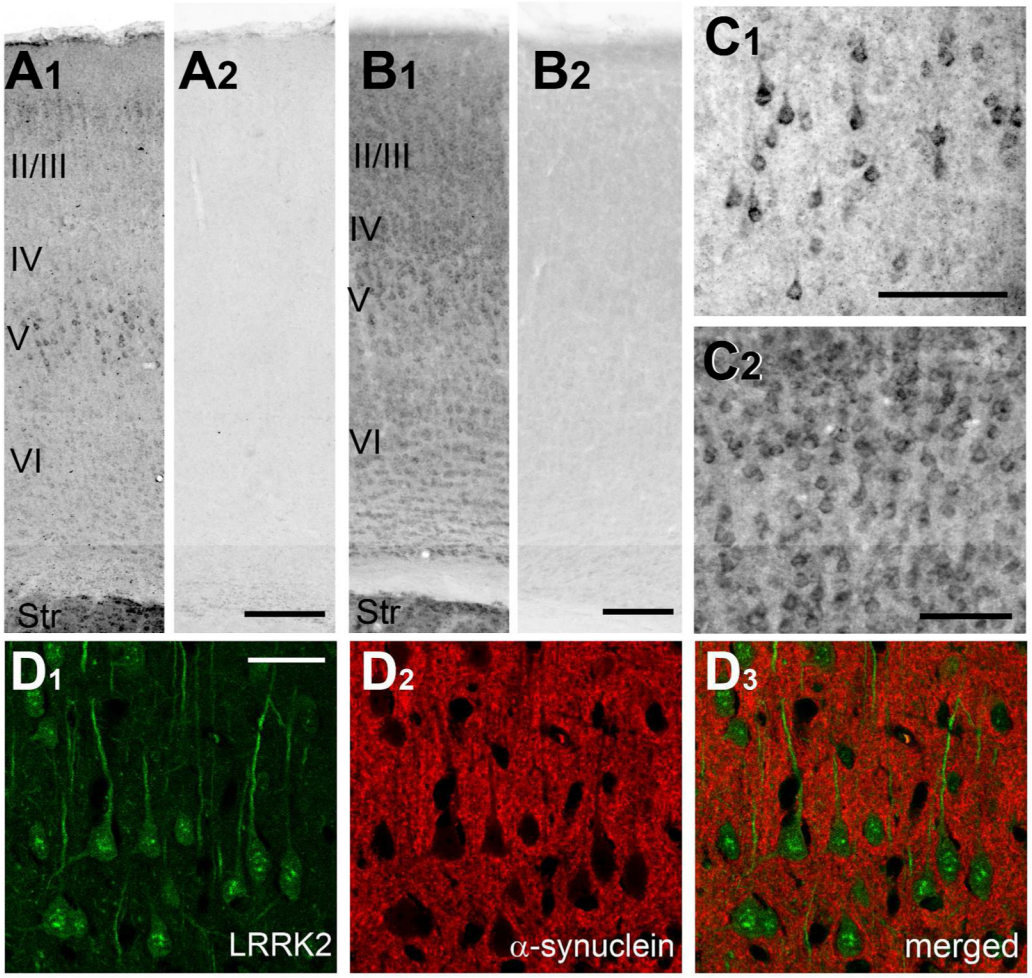

Figure 3. LRRK2 in adult rodent cortex

A) LRRK2 distribution using DAB-immunohistochemistry in wild type rat motor cortex (panel A1) and LRRK2 KO rat motor cortex (panel A2) with monoclonal antibody N241A/34. Scale bars are 0.3 mm. **B)** Wild-type mouse motor cortex (panel B1) and LRRK2 KO mouse motor cortex (panel B2) with monoclonal antibody c41-2. Scale bars are 0.15 mm for mouse. Cortical layering was defined by cresyl violet staining (not shown). **C)** Higher magnification of cortical Layer V in rat (panel C1) and mouse (panel C2) demonstrate a more restricted expression pattern of LRRK2 in rat compared to mouse. Scale bar is 0.15 mm for rat (panel C1) and 75 μm for mouse (panel C2). **D)** Immunofluorescence with antibody N241A/34 in rat cortex layer V using confocal microscopy demonstrate a prominent somatodendritic localization of LRRK2 in Layer V of the cortex, although possible LRRK2 expression in non-branching, non-tapering axons cannot be ruled out through these images. LRRK2 also localizes to perinuclear puncta. LRRK2 does not co-localize with the presynaptic marker, α –synuclein, which demarcates LRRK2 positive apical dendrites. Scale bar is 25 μm for all panels in D. A magenta-green version of the images is available as Supplemental Figure 3.

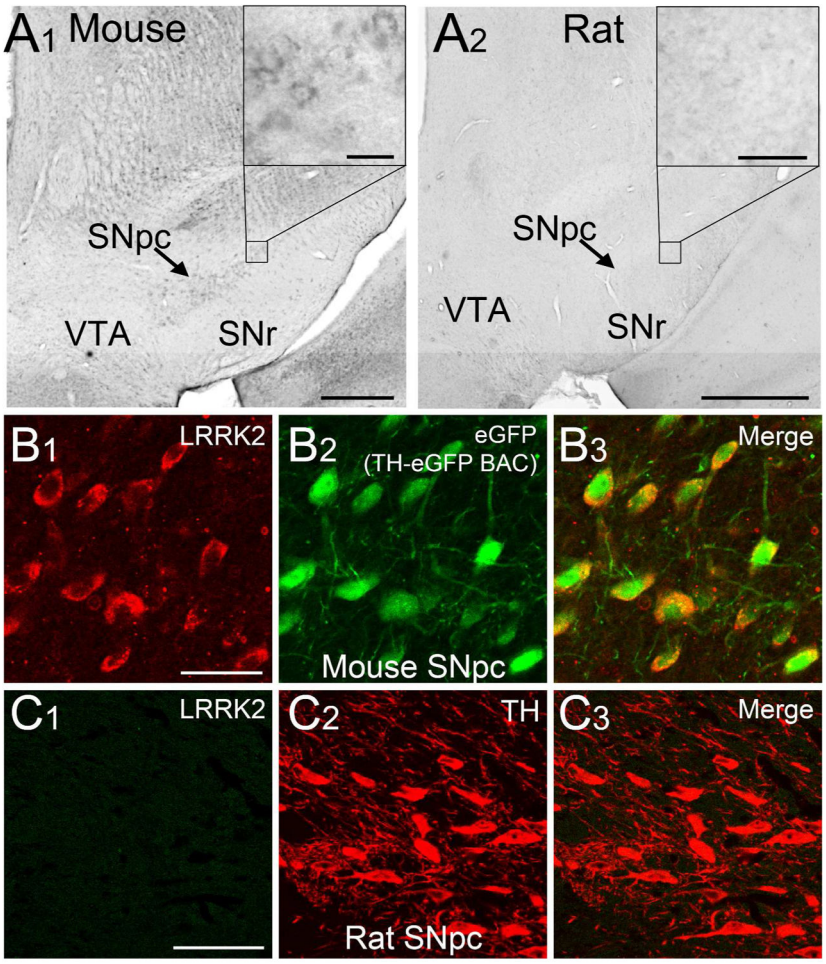

Figure 4. LRRK2 in rodent SNpc

A) LRRK2 using DAB immunohistochemistry in adult male rats or mice with the substantia nigra pars compacta (SNpc), substantia nigra pars reticulata (SNr), and Ventral Tegmental Area (VTA) indicated. No specific signal was obtained in simultaneously processed mouse LRRK2 KO tissue. Results are shown using antibody c41-2. LRRK2 immunoreactivity could be seen in mouse sections, but not in rat using either c41-2 antibody or N241A/34 monoclonal antibody(shown). Scale bars are 0.5 mm, inset scale bars are 50 μm. **B)** A strain of mouse produced by the GeneSat project that expresses eGFP under the endogenous TH promoter from a BAC construct (see Methods) was used to evaluate LRRK2 in the mouse midbrain. eGFP epifluorescence could be visualized in the SNpc, and these cells were positive for LRRK2 protein. Scale bar is 30 μm. **C)** At a comparable level of the SNpc in rats, robust TH expression could be observed but none of these cells were LRRK2 positive using antibodies N241A/34 (shown) or c41-2. Scale bar is 50 μm. A magenta-green version of the images is available as Supplemental Figure 4.

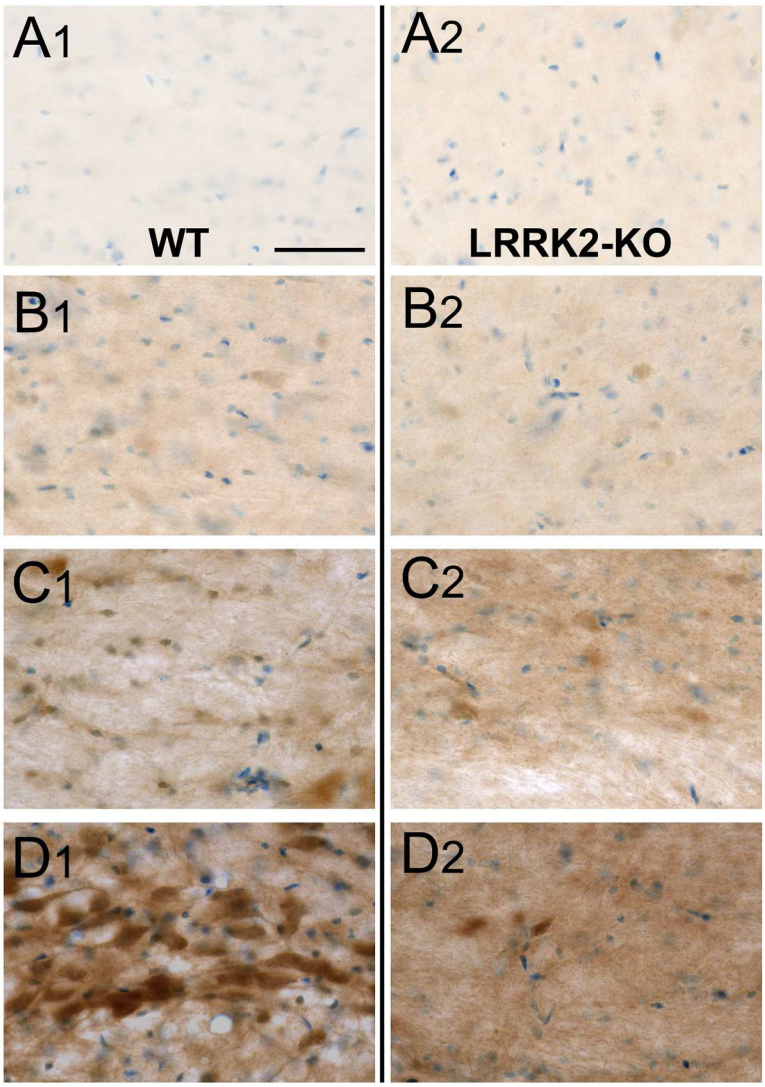

Figure 5. Titration of anti-LRRK2 antibodies in the rat SNpc

SNpc from adult WT (left panels, labeled subpanels 1) and LRRK2 KO rats (right panels, labeled subpanels 2), with increasing concentrations of primary antibody (N241A/34) at **A)** 1 μg/ml (standard concentration used in all other experiments), **B)** 2.5 μg/ml **C)** 13 μg/ml and **D)** 40 μg/ml, together with secondary antibody held at 1 μg/ml for all panels. Nissl stain was provided to aid in the identification of the SNpc. The lateral SNpc is shown for all panels, with both LRRK2 WT and LRRK2 KO sections processed in parallel. Scale bar is 40 μm for all panels.

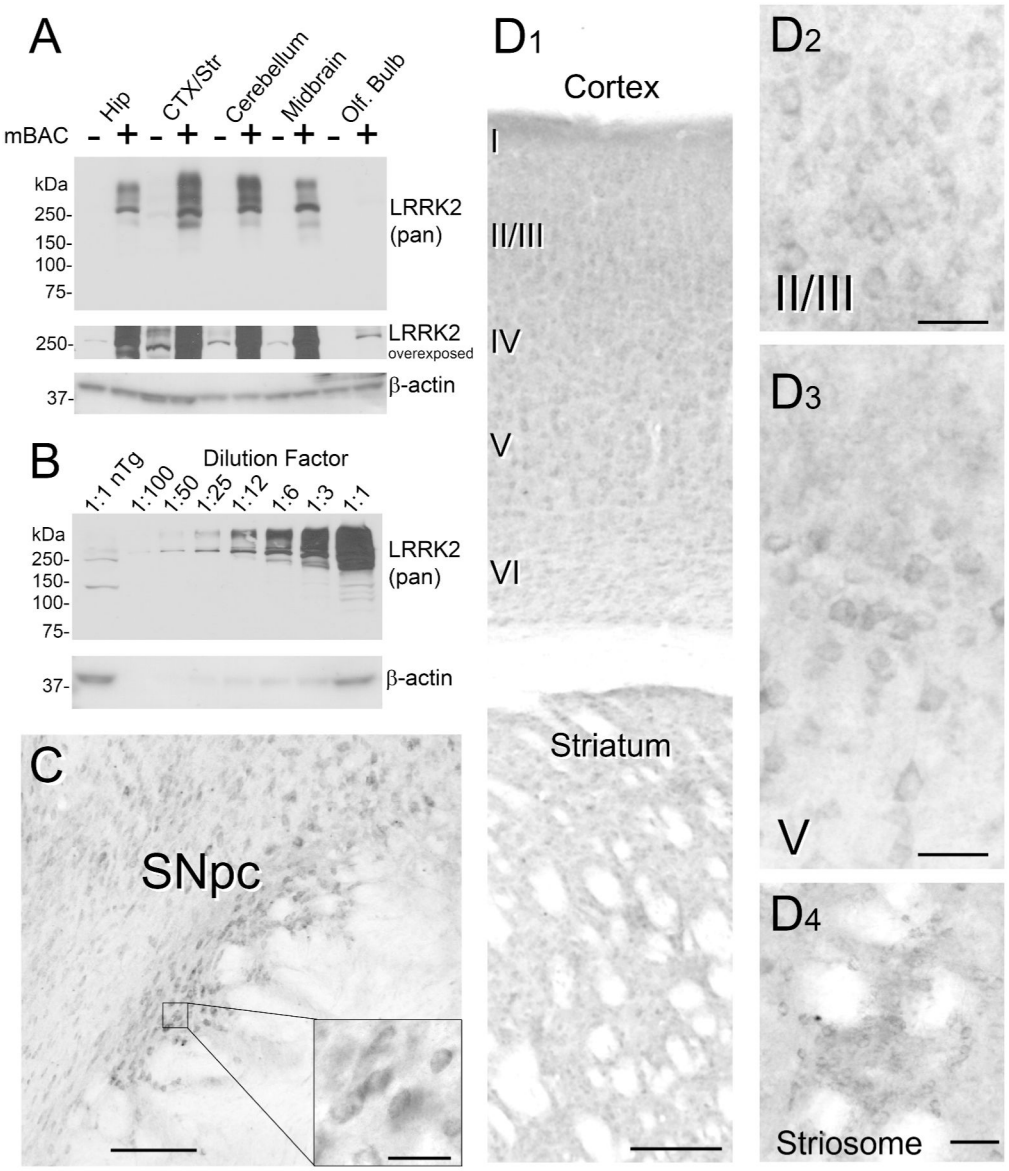

Figure 6. Mouse LRRK2 BAC Transgenic Expression Mimics Endogenous Distribution

A) Western blot analysis with antibody N241A/34 demonstrating the level of overexpression in the indicated brain region, as dissected from fresh mouse brain tissue from either nontransgenic or LRRK2-G2019S BAC transgenic mice. Equivalent protein concentrations determined by BCA assay were loaded between lanes, matched by region, between wild-type and transgenic mice. **B)** Forebrain lysate from nontransgenic mice was loaded in lane 1, and increasing concentrations of LRRK2-G2019 transgenic mouse forebrain lysates were loaded in subsequent lanes. LRRK2 is overexpressed between 25 and 50 fold in the transgenic rats. **C,D**) LRRK2, as detected in adult male mice with antibody c41-2 using DAB immunohistochemistry in the SNpc (Panel C) and in the anterior striatum and motor cortex (panel D). Scale bars are 0.2 mm and 40 μm for panel C and inset, respectively. Scale bars are 200 μm for panel D1, 40 μm for panel D2 and D3, and 100 μm for panel D4.

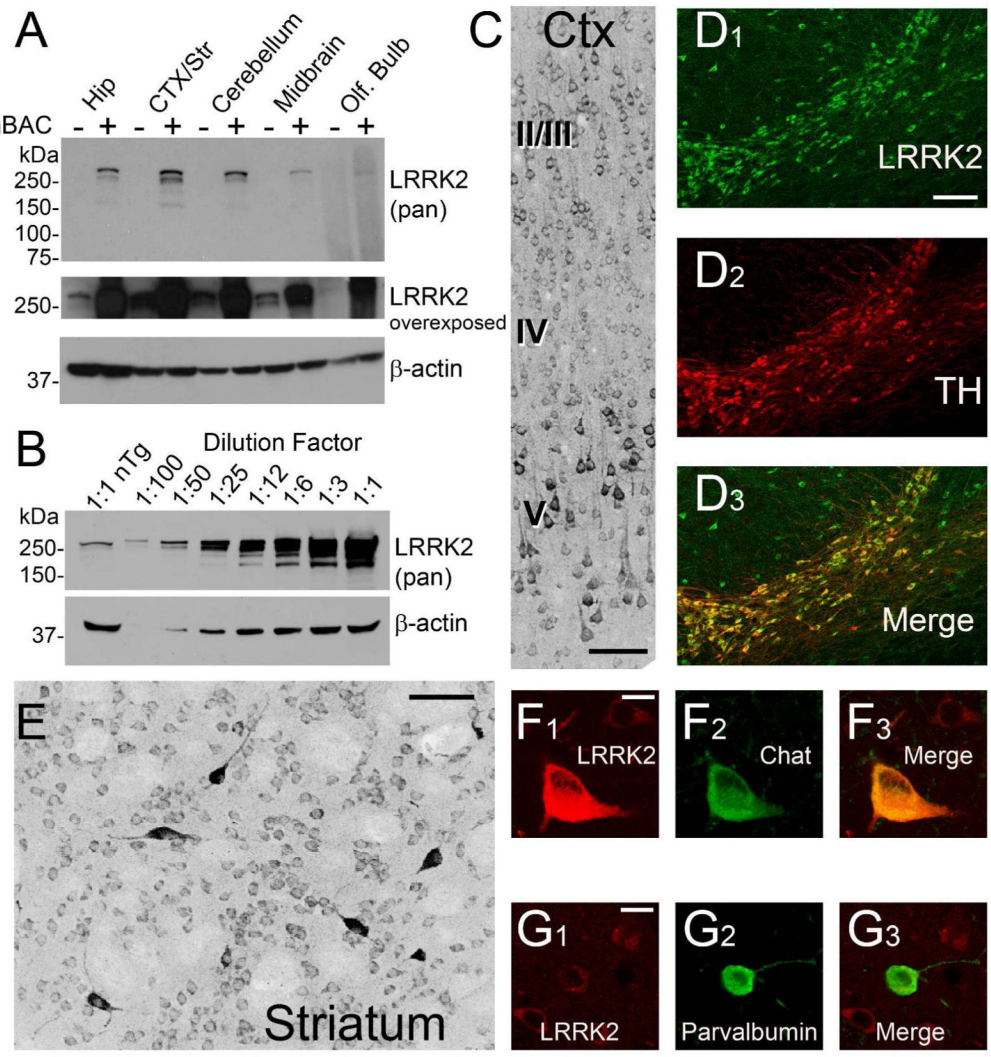

Figure 7. Aberrant LRRK2 Distribution Caused by Expression of Human LRRK2 BAC Constructs in Rats

A) Western blot analysis with antibody N241 demonstrating the level of LRRK2 overexpression in the indicated brain region, as dissected from fresh rat brain tissue from either nontransgenic or LRRK2-G2019S human-BAC transgenic rats. Equivalent protein concentrations determined by BCA assay were loaded between lanes (and verified by actin signal), matched by region, between wild-type and transgenic rats. **B)** Forebrain lysate from nontransgenic rats was loaded in lane 1 and increasing concentrations of LRRK2-G2019S transgenic rat forebrain lysates were loaded in subsequent lanes. LRRK2 is overexpressed between 25 and 50 fold in the transgenic rats. **C)**The pan-reactive LRRK2 antibody N241A/34 was used to detect LRRK2 in LRRK2-G2019S hBAC positive rats in the motor cortex (scale bar is 50 μm), and **D)** SNpc, by fluorescent co-label with TH (scale bar is 0.1 mm). **E)** A striosome in the anterior striatum of transgenic rats identified by LRRK2, with intensely positive LRRK2 interneurons inside the striosome (scale bar is 50 μm. **F,G**) Co-localization of LRRK2 with cholinergic interneurons, but weak expression in parvalbumin-

positive interneurons (scale bars are 10 μm). A magenta-green version of the images is available as Supplemental Figure 5.

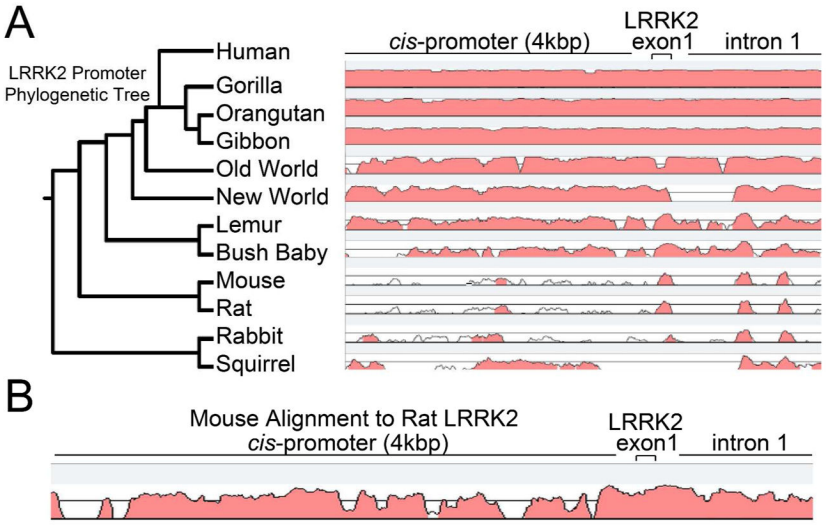

Figure 8. Lack of Conservation of LRRK2 Regulatory Regions in Mammals

A) A block of sequence from the human genome (GRCh37/hg19) encompassing 4 kbp upstream of the LRRK2 transcription start site in the brain (mapped previously (West et al., 2005)) and 1kbp downstream of exon 1 was analyzed by mVISTA alignment software together with the equivalent block of sequence from the indicated mammalian species, using the conserved exon 1 sequence (and LRRK2 translational start sequence, within) as an anchor. A computed phylogenic tree was assigned (mVISTA) that closely matched the expected species genomic phylogeny. A shuffle-LAGAN alignment detected regions of sequence conservation (shown as a pink-filled histogram). Global alignments were also performed against the indicted species to ensure the shuffle-LAGAN alignment was performed on the region with highest homology. **B)** LAGAN alignment of the mouse and rat regulatory regions in LRRK2.

Table 1

List of antibodies utilized in this study.

Primary Antibody/ Clone Name	Immunogen	Catalog Number	Source	Host species /Isotype/Mono or Polyclonal
anti-LRRK2 c41-2	Recombinant protein 970-2527AA of human LRRK2	3514-1	Epitomics	Rabbit/IgG1/Monoclonal
anti-LRRK2 N241A/34	Recombinant protein 970-2527AA of human LRRK2	73-253	NeuroMab	Mouse/IgG2a/Monoclonal
anti-Calbindin	Recombinant protein 1-150AA of human Calbindin	2946-1	Epitomics	Rabbit/IgG1/Monoclonal
anti-MOR-1	Recombinant protein 250-400AA of human MOR-1	3675-1	Epitomics	Rabbit/IgG1/Monoclonal
anti-GAD67	Recombinant full length human GAD67	MAB5406	Millipore	Mouse/IgG2a/Monoclonal
anti-Parvalbumin	Parvalbumin purified from frog muscle	MAB1572	Millipore	Mouse/IgG1/Monoclonal
anti-TH	Recombinant protein 1-196AA of human TH	H-196	Santa Cruz	Rabbit/IgG/Polyclonal
anti-α-Synuclein	Recombinant protein 15-123AA of rat synuclein	610785	BD Biosci	Mouse/IgG1/Monoclonal
anti-Choline Acetyltransferase	Choline Acetyltransferase purified from human placenta	AB144P	Millipore	Goat/IgG/Polyclonal
anti-DARPP-32	Synthetic peptide to residues surrounding 160AA of human DARPP-32	2306	Cell Signaling	Rabbit/IgG/Polyclonal